

## Wearable Contact Lens Ultrasound Retinal Stimulation for Noninvasive Vision Restoration

*Chi-feng Chang<sup>1</sup>, Jie Ji<sup>1</sup>, Yushun Zeng<sup>1</sup>, Baoqiang Liu<sup>2</sup>, Junhang Zhang<sup>1</sup>, Xin Sun<sup>1</sup>, Gong Chen<sup>1</sup>, Hamid Chabok<sup>3</sup>, and Qifa Zhou<sup>1,2</sup>*

<sup>1</sup>*University of Southern California, Department of Biomedical Engineering, Los Angeles, California, USA*

<sup>2</sup>*University of Southern California, Roski Eye Institute, Keck School of Medicine, Los Angeles, California, USA*

<sup>3</sup>*University of Southern California, Department of Physics and Astronomy, Los Angeles, California, USA*

**Abstract:** This work presents the first wearable, contact lens-compatible ultrasound neuromodulation device capable of precise retinal stimulation without surgery. A novel wearable contact lens-shaped ultrasound array is designed for potential vision restoration in retinal degenerative diseases through noninvasive neuromodulation. The array is integrated by 64 elements on a biocompatible substrate, aiming for ~100–150  $\mu\text{m}$  resolution. The fabrication process utilizes a 3D-printed mold, silver epoxy, flexible PCB, and Parylene-C coating to create a device operating at 19.5 MHz with over 50% bandwidth. The Field-Programmable Gate Array (FPGA) control supports real-time programmable patterns for high-precision neuromodulation. In contrast to invasive options, this approach minimizes risks and enhances resolution, showing great potential in vision therapy.

**Keywords:** Retinal stimulation, focused ultrasound, contact lens, vision restoration, noninvasive neuromodulation

### Background, Motivation and Objective

Retinal degenerative diseases, including age-related macular degeneration and retinitis pigmentosa, affect over 200 million people globally, causing irreversible blindness due to photoreceptor loss [1-3]. The intact inner retinal circuitry supports prosthetic interventions, yet current solutions like the FDA-approved Argus II rely on invasive electrodes, posing surgical risks and offering limited resolution (~200–300  $\mu\text{m}$ ) [1, 4, 5]. Noninvasive neuromodulation, such as transcranial magnetic stimulation, lacks precision, while optogenetics and sonogenetics involve genetic risks [6]. Focused ultrasound (FUS) offers a promising alternative with ~100  $\mu\text{m}$  resolution and minimal thermal effects [2, 3]. Previous studies [2, 5, 7] demonstrated FUS potential in ultrasound neuromodulations, with Lu et al. advancing imaging-guided systems. Despite progress, wearable FUS devices remain limited. We developed a contact lens-shaped transducer with a 64-element PZT array, using a 3D-printed mold, silver epoxy, flexible PCB, and Parylene-C coating for ~100–150  $\mu\text{m}$  resolution and FPGA-controlled patterning [1, 8]. Our goal is to achieve a noninvasive, high-precision, biocompatible vision restoration solution, overcoming implant

limitations, with future potential for direct integration into the eye as a wearable contact lens [9].

### Method

#### Design

The contact lens-shaped ultrasound transducer is designed for high-resolution, noninvasive retinal stimulation, featuring a 64-element PZT phased array in a dual-ring configuration: 32 elements in an inner ring (OD 14 mm, ID 12 mm) and 32 in an outer ring (OD 17 mm, ID 15 mm), mounted on a flexible PCB (OD 20 mm, ID 9 mm) with a focal length of 18 mm. The PZT (DL-53) 1-3 composite (DeL Piezo Specialties, LLC), with a longitudinal velocity of ~3087 m/s and impedance of 16–18 MRayl, ensures flexibility and broadband performance, supporting stable operation under extreme conditions. A silver epoxy and Parylene-C matching layers enhance acoustic coupling and biocompatibility, while the design minimizes lens heating (Fig. 1), making it suitable for prolonged ocular use. This configuration is optimized for future direct placement on the eye, mimicking a standard contact lens for seamless wearability.

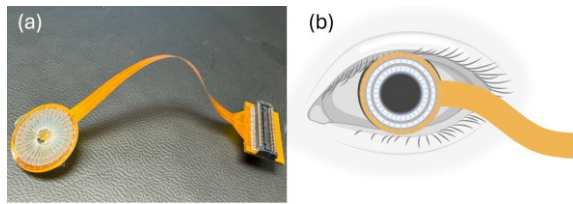


Fig. 1: (a) Contact lens-shaped ultrasound array. (b) Conceptual illustration of the intended wearing method.

#### Fabrication

A 3D-printed concentric mold (Fig. 2) shapes the dual-ring array, aligning with ocular curvature for a 64-element PZT array (inner ring: OD 14 mm, ID 12 mm; outer ring: OD 17 mm, ID 15 mm) on a PCB (OD 20 mm, ID 9 mm). The PZT (DL-53) 1-3 composite (longitudinal velocity  $\sim 3087$  m/s, impedance 16–18 MRayl) is placed in the mold, with a silver epoxy matching layer cast on the front and an E-solder backing layer on the rear for connectivity and damping. Segmented fabrication ensures layer uniformity. The PZT is diced into 64 elements at  $11.25^\circ$  spacing rotation, with epoxy-filled gaps for integrity, mounted on the PCB, and fitted with Cr/Au electrodes [10–12]. A Parylene-C coating adds biocompatibility, and epoxy resin fixes the 18 mm focal length for ocular conformity [13]. A single cable connects to the control system, with wireless designs planned. The final fabricated device is a compact, biocompatible contact lens-shaped transducer ready for potential direct ocular integration, as shown in the post-fabrication images (Fig. 2).

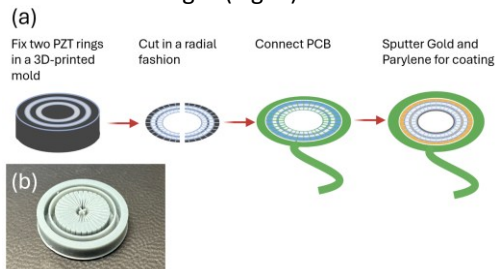


Fig. 2: (a) Completed transducer assembly. (b) 3D-printed mold with radial cutting guides.

#### Simulation and Control

PiezoCAD (Sonic Concepts, Inc.) was applied to design and optimize the array in a central frequency of 19.5 MHz (PZT thickness  $\sim 0.079$  mm),  $-6$  dB bandwidth of 81.3%, showcasing the DL-53 1-3 composite's potential in higher stimulation resolution (Fig. 3) [14–16]. The dual-ring design, with a 3087 m/s velocity and  $\sim 17$  MRayl impedance, optimized focusing for  $\sim 100$ – $150$   $\mu\text{m}$  resolution. FPGA control enabled real-time beam steering and holography-based patterning, leveraging holographic principles to create complex spatial acoustic patterns by modulating phase and amplitude delays across array elements. This

capability supports the future development of direct eye-wearable systems for retinal stimulation.

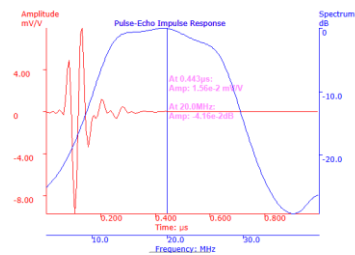


Fig. 3: Pulse-Echo Impulse Response ( $-6$  dB Bandwidth: 81.3%) by simulation.

#### Wearable 64-Ch Neuromodulation System

The system consists of a 64-channel ultrasound transmitter (TX7364), a low-power FPGA (XC7A100T), and a Wi-Fi module for wireless communication, all powered by a capacitor-based energy storage module (Fig. 4). The high-voltage rail delivers programmable output up to 60 Vpp, enabling the system to drive a 19.5 MHz ring array transducer for targeted therapeutic ultrasound stimulation. The low-voltage rail powers the control logic and communication components. The FPGA offers dynamic and real-time control of individual channel delays, allowing precise adjustment of acoustic focus and stimulation depth. This per-channel programmability enables spatially selective neuromodulation and improves adaptability across anatomical targets. The system supports ultrasound frequencies up to 22 MHz, making it suitable for high-frequency neuromodulation and advanced biomedical research. Wireless communication is supported by a dual-band Wi-Fi module with data transfer rates up to 450 Mbps, ensuring seamless connection to mobile devices or cloud platforms. A 16,000  $\mu\text{F}$  capacitor-based energy storage module ensures stable high-voltage pulse delivery during extended operation, providing both performance and reliability in wearable applications.

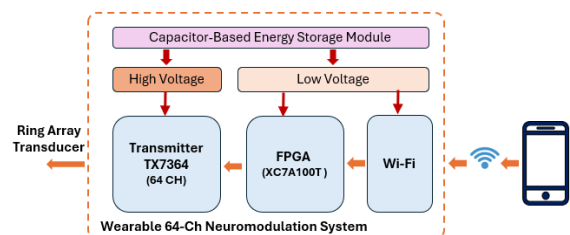


Fig. 4: Block diagram of the wearable 64-channel neuromodulation system.

#### Experimental Results

##### Safety Validation

The contact lens-shaped ultrasound transducer underwent a 20-hour safety test, operating continuously at 50 V under extreme conditions, and exhibited reliable thermal and acoustic performance suitable for potential direct ocular integration. All tests were conducted in compliance with FDA

guidelines for ophthalmic ultrasound safety, ensuring the mechanical index (MI) remains below 0.23 [17]. Post-fabrication analysis of the device's thermal behavior, based on the 64-element PZT dual-ring array, reveals a baseline temperature of approximately 20°C prior to stimulation. During maximum stimulation at 50 V, the temperature rises to around 25°C, indicating controlled heat generation within safe limits for prolonged ocular use. Following the 20-hour test, the temperature stabilizes at approximately 22°C (Fig. 5), suggesting effective thermal regulation and confirming the device's biocompatibility.

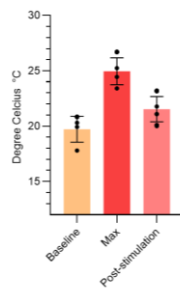


Fig. 5: Thermal Performance Analysis of the Ultrasound Ring Array in a 20-Hour Safety Test.

Acoustic performance under the same 50 V maximum input condition was evaluated, yielding an output voltage of 26.04 mV, a receive-mode sensitivity of  $4.26 \times 10^{-8}$  V/Pa, and a sensitivity of  $2.72 \times 10^{-5}$  V<sup>2</sup>cm<sup>2</sup>/W. The spatial peak pulse average intensity ( $I_{\text{sp}}^{\text{ppa}}$ ) was measured at 24.92 W/cm<sup>2</sup>. The acoustic pressure (P) was calculated as Eq. (1) and determined to be 0.3056 MPa:

$$P = \frac{\text{Output}}{2 \times \text{Sensitivity} \left( \frac{\text{V}}{\text{Pa}} \right) \times 10^6} \quad (1)$$

The mechanical index (MI) was calculated using Eq. (2):

$$MI = \frac{\text{Pressure (MPa)}}{\sqrt{\text{Frequency (MHz)}}} \quad (2)$$

According to Eq. (2), the MI is 0.068, well below the FDA ophthalmic safety threshold of 0.23. These results support the device's readiness for future in vivo validation and seamless integration as a wearable contact lens under extreme operational conditions

### Discussion

This study introduces a contact lens-shaped ultrasound transducer as a noninvasive alternative to retinal prostheses, with a fabrication process emphasizing biocompatibility and ocular conformity for potential direct placement in the eye [18]. The 19.5 MHz frequency, resulting from the combined resonance of the PZT, silver epoxy, and E-solder layers, supports high-resolution (~120 μm) stimulation [2, 7]. Unlike the Argus II's invasive approach, our design eliminates surgical risks and improves

biocompatibility [4]. The dual-ring configuration, inspired by Jiang et al.'s F-URSP [7], supports programmable patterns, with FPGA control building on Lu et al.'s imaging-guided systems [5]. The device underwent a 20-hour safety test under extreme conditions with a maximum input voltage of 50 V, demonstrating stable thermal performance with a maximum temperature of 25°C and a post-stimulation stabilization at 22°C, indicating effective thermal regulation for prolonged ocular use. Acoustic performance under the same conditions yielded a mechanical index (MI) of 0.068, well below the FDA ophthalmic safety threshold of 0.23, confirming its safety for neuromodulation. This reliability under high-load conditions underscores the device's potential for future clinical applications.

Future work will address in vivo validation to assess neural responses, long-term biocompatibility to ensure sustained ocular safety, and wireless power challenges to enhance wearability [19]. These advancements could transform vision restoration therapy through a truly wearable, contact lens-integrated device, offering a safe and precise alternative to existing invasive solutions.

### Acknowledgements

The project was partially supported by NIH NEI STTR 1R41EY035609-01.

### References

- [1] C. Xu et al., "Design and Simulation of a Ring Transducer Array for Ultrasound Retinal Stimulation," *Micromachines*, vol. 13, no. 9, 2022, doi:10.3390/mi13091536.
- [2] Q. X et al., "Noninvasive Ultrasound Retinal Stimulation for Vision Restoration at High Spatiotemporal Resolution," *BME Frontiers*, 2022, doi:10.34133/2022/9829316.
- [3] G. Lu et al., "Ultrasound retinal stimulation: a mini-review of recent developments," *IEEE Transactions on Ultrasonics, Ferroelectrics, and Frequency Control*, vol. 69, no. 12, 2022, doi:10.1109/TUFFC.2022.3220568.
- [4] J.-y. Lu, G. Lu, B. B. Thomas, M. S. Humayun, and Q. Zhou, "Ultrasound Concave 2-D Ring Array for Retinal Stimulation," *IEEE Transactions on Ultrasonics, Ferroelectrics, and Frequency Control*, vol. 70, pp. 1527-1535, 2023, doi:10.36227/techrxiv.22083719.
- [5] G. Lu et al., "Noninvasive imaging-guided ultrasonic neurostimulation with arbitrary 2D patterns and its application for high-quality vision restoration," *Nature Communications*, vol. 15, no. 1, 2024, doi:10.1038/s41467-024-48683-6.
- [6] P.-A. Lo et al., "Ultrasonic Retinal Neuromodulation and Acoustic Retinal Prosthesis," *Micromachines*, vol. 11, no. 10, 2020, doi:10.3390/mi11100929.

- [7] L. Jiang et al., "Flexible ultrasound-induced retinal stimulating piezo-arrays for biomimetic visual prostheses," *Nature Communications*, vol. 13, no. 1, 2022, doi:10.1038/s41467-022-31599-4.
- [8] W. Qiu et al., "A novel dual-frequency imaging method for intravascular ultrasound applications," *Ultrasonics*, vol. 57, 2015, doi:10.1016/j.ultras.2014.10.011.
- [9] C. Gong et al., "Non-Invasive Hybrid Ultrasound Stimulation of Visual Cortex In Vivo," *Bioengineering*, vol. 10, no. 5, 2023, doi:10.3390/bioengineering10050577.
- [10] L. B et al., "A Novel Dual-Element Catheter for Improving Non-Uniform Rotational Distortion in Intravascular Ultrasound," *IEEE Transactions on Biomedical Engineering*, vol. 70, no. 6, 2023, doi:10.1109/TBME.2022.3226955.
- [11] B. L. M. S. Z. L. S. Y. Y. W. Qiu, "A Novel Coded Excitation Imaging Platform for Ultra-High Frequency (>100 MHz) Ultrasound Applications," *IEEE Transactions on Biomedical Engineering*, vol. 72, no. 4, 2025, doi:10.1109/TBME.2024.3496843.
- [12] Y. Chen et al., "Focused intravascular ultrasonic probe using dimpled transducer elements," *Ultrasonics*, vol. 56, 2015, doi:10.1016/j.ultras.2014.07.011.
- [13] S. Liang et al., "Evaluation of Blood Induced Influence for High-Definition Intravascular Ultrasound (HD-IVUS)," *IEEE Transactions on Ultrasonics, Ferroelectrics, and Frequency Control*, vol. 69, no. 1, 2022, doi:10.1109/TUFFC.2021.3108163.
- [14] M. Su et al., "High frequency focal transducer with a Fresnel zone plate for intravascular ultrasound," *Applied Physics Letters*, vol. 119, no. 14, 2021, doi:10.1063/5.0070313.
- [15] Z. Y et al., "High-Frequency Wearable Ultrasound Array Belt for Small Animal Echocardiography," *IEEE Transactions on Ultrasonics, Ferroelectrics, and Frequency Control*, vol. 71, no. 12, 2024, doi:10.1109/TUFFC.2024.3492197.
- [16] C. Qiu et al., "Textured-piezoelectric-ceramic-based focused intravascular ultrasonic transducer with improved image quality and uniformity," *Applied Physics Letters*, vol. 125, no. 23, 2024, doi:10.1063/5.0237897.
- [17] FDA, "Marketing Clearance of Diagnostic Ultrasound Systems and Transducers," 2023. Available: <https://www.fda.gov/regulatory-information/search-fda-guidance-documents/marketing-clearance-diagnostic-ultrasound-systems-and-transducers>.
- [18] H. Caffaratti et al., "Neuromodulation with Ultrasound: Hypotheses on the Directionality of Effects and Community Resource," *medRxiv*, 2025, doi:10.1101/2024.06.14.24308829.
- [19] J. Ji et al., "Potential of ultrasound stimulation and sonogenetics in vision restoration: a narrative review," *Neural Regeneration Research*, vol. 20, no. 12, 2025, doi:10.4103/NRR.NRR-D-24-00841.